ELSEVIER

Biochimica et Biophysica Acta 1460 (2000) 192–203

BIOCHIMICA ET BIOPHYSICA ACTA
BBA

www.elsevier.com/locate/bba

Review

Water and bacteriorhodopsin: structure, dynamics, and function

Norbert A. Dencher [a,*], Hans Jürgen Sass [b], Georg Büldt [b,1]

[a] *Technische Universität Darmstadt, Institute of Biochemistry, Physical Biochemistry, Petersenstrasse 22, D-64287 Darmstadt, Germany*
[b] *Forschungszentrum Jülich, IBI-2, Institute for Structural Biology, D-52425 Jülich, Germany*

Received 24 March 2000; accepted 24 March 2000

Abstract

A wealth of information has been gathered during the past decades that water molecules do play an important role in the structure, dynamics, and function of bacteriorhodopsin (bR) and purple membrane. Light-induced structural alterations in bR as detected by X-ray and neutron diffraction at low and high resolution are discussed in relationship to the mechanism of proton pumping. The analysis of high resolution intermediate structures revealed photon-induced rearrangements of water molecules and hydrogen bonds concomitant with conformational changes in the chromophore and the protein. These observations led to an understanding of key features of the pumping mechanism, especially the vectoriality and the different modes of proton translocation in the proton release and uptake domain of bR. In addition, water molecules influence the function of bR via equilibrium fluctuations, which must occur with adequate amplitude so that energy barriers between conformational states can be overcome.

Keywords: Bacteriorhodopsin; Proton pumping; Photocycle; Purple membrane; Neutron scattering; X-Ray diffraction

1. Water molecules: necessary elements for proton translocation by bacteriorhodopsin

The photon-driven proton pump bacteriorhodopsin (bR) in the purple membrane (PM) of Haloarchaea is *the* prototype of an integral membrane protein, especially of the family of seven membrane-spanning α-helical proteins. At present, bR is one of the best characterized active ion-translocating proteins. In the near future, it will be the first membrane protein whose vectorial transport mechanism is understood at the atomic level.

An advantage of bR is the possibility to monitor the kinetics and stoichiometry of proton pumping by flash absorption spectroscopy in combination with optical pH indicators [1,2]. In this way, it was shown that only one proton per cycling bR is released during the first part of the photocycle [2–6]. From spectroscopic data the occurrence of conformational changes during the BR to M transition was suggested [1,4]. Although bR is arranged in the PM as a lattice of trimers in a two-dimensional hexagonal crystal, the bR monomer itself is the functional unit for proton pumping [6,7]. By employing optical pH indicators bound selectively to both membrane surfaces [5,8–14] vectorial proton transfer steps across bR and along the membranes surface can be examined, as illustrated in Fig. 1. H^+ transfer processes from

Abbreviations: bR, bacteriorhodopsin; PM, purple membrane; BR, light-adapted ground state of bR; wt, wild-type; r.h., relative humidity

* Corresponding author. Fax: +49 (6151) 164171; E-mail: dencher@pop.tu-darmstadt.de

[1] Also corresponding author. Fax: +49 (2461) 612030; E-mail: g.bueldt@fz-juelich.de

0005-2728/00/$ – see front matter
PII: S0005-2728(00)00139-0

the active centre of bR to the extracellular side (Fig. 1A, reaction 1) and from there along the membrane-water interphase to the cytoplasmic side of bR (reaction 2) are kinetically and spatially resolved. In Fig. 1B, the respective absorbance changes upon light excitation are plotted on a logarithmic time scale covering seven decades. The upper trace (M) represents rise and decay of the photocycle intermediate M, which plays a major role in the proton pumping process. The lower traces are absorbance changes of the pH indicators fluorescein (F) bound to K129 at the extracellular surface of bR and of pyranine (P) which resides in the aqueous bulk phase (Fig. 1A). Upon light excitation, concomitant with the rise of the M intermediate ($\tau_{mean} = 83$ μs at 20°C), a proton is pumped from the interior of bR (RH^+, reaction 1) to the extracellular surface where it is detected by fluorescein ($\tau = 90$ μs). The pumped proton dwells for about 1 ms at the membrane surface (reaction 2) before it is released into the aqueous bulk phase ($\tau = 830$ μs, as monitored by fluorescein, reaction 3) and is detected by pyranine ($\tau = 1100$ μs, reaction 3). Proton reuptake necessary to complete proton cycle and photocycle (reaction 4), is monitored by the relaxation of the absorbance changes of both pH indicators to the initial value (pyranine: $\tau = 6.7$ ms, fluorescein: $\tau = 10.4$ ms), just after the decay of the M intermediate ($\tau_{mean} = 5.0$ ms, Fig. 1B). Under physiological conditions, the cytoplasmic surface of bR has to pick up protons from the well-buffered, slightly alkaline cytoplasmic matrix. Attraction of protons from the medium and funnelling these protons into the orifice of the cytoplasmic proton channel are enhanced by a cluster of exposed carboxylates, acting as proton-collecting antenna [13,15,16]. A contradicting view, however, is presented by Brown et al. [17].

Very early, the influence of water on the photocycle kinetics and on charge movements in bR has been observed [1,4,18,19] and previously studied in great detail [20–27]. The functional importance of water molecules for bR is clearly demonstrated in Fig. 1C, illustrating the dependence of the kinetics of the intermediate M as well as the kinetics and efficiency of proton pumping on the relative humidity. Both the decay of M (but not its formation) and the regeneration of the ground state are strongly slowed down below 80% relative humidity (r.h.) (compare Fig. 1B and C). As measured with the optical pH indicator pyranine, the proton pumping activity is decreased below 70% r.h. and no activity is observed below about 50% r.h., although there is still a – very slow – photocycle (Fig. 1C). At the same threshold value of about 60–50% r.h., where proton transport stops, also the light-induced conformational changes in the protein vanish [20] (see below). All these properties of bR, i.e., the photocycle, the proton pumping cycle, and the conformational changes are influenced by the extent of hydration, proving the functional importance of water.

A first glance on the structural basis for the observed participation of water in the function emerged from neutron diffraction experiments in which the water distribution in projection on the PM plane at different r.h. was determined by $H_2O/^2H_2O$ exchange experiments [28]. A dominant difference density peak corresponding to 6–8 water molecules [29] was detected in the central part of the projected structure of bR in the vicinity of the Schiff base end of the chromophore (SB, Fig. 2) [28,30]. The water molecules are very strongly associated with the protein [28]. These water molecules together with exchangeable hydrogens were suggested to be elements of the active centre as well as to provide the conductance pathway for protons connecting the active centre with both surfaces of the membrane.

A further outcome of the neutron diffraction investigation is the finding that at high hydration, the lipid head group region of the membrane surface is more hydrated than the protein [28,30]. The hydration water of the PM surface has peculiar properties. For example, freezing of water occurs several degrees below the freezing point of bulk water (supercooled membrane water) and the first surface layer does not transform into the crystalline state, even below 240 K ('nonfreezing water') [31,32]. Water molecules at the PM surface show anisotropic (only parallel to the membrane plane) two-dimensional long-range translational diffusion ($D_s = 4.4 \times 10^{-6}$ cm^2/s), about five times slower than in bulk water [33,34]. Translational diffusion in the direction perpendicular to the PM surface is not observable during the time window of the neutron scattering measurement. This extraordinary behaviour of the surface hydration water in combination with the high buffer capacity of bR and lipid head groups [10,35] might be the reason for the

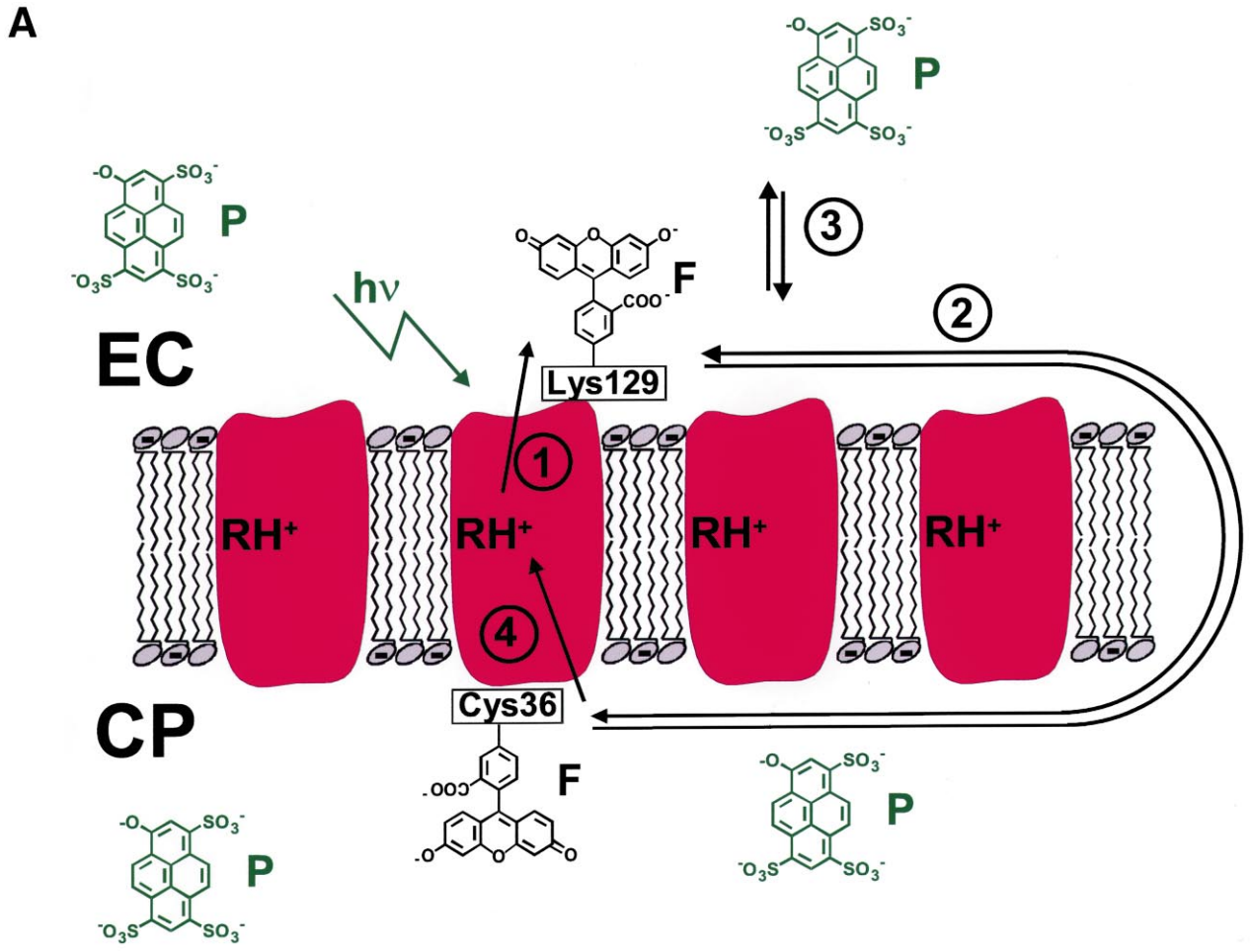
A
P
P
P
P
hν
F
F
EC
CP
Lys129
Cys36
RH+
RH+
RH+
RH+
1
2
3
4

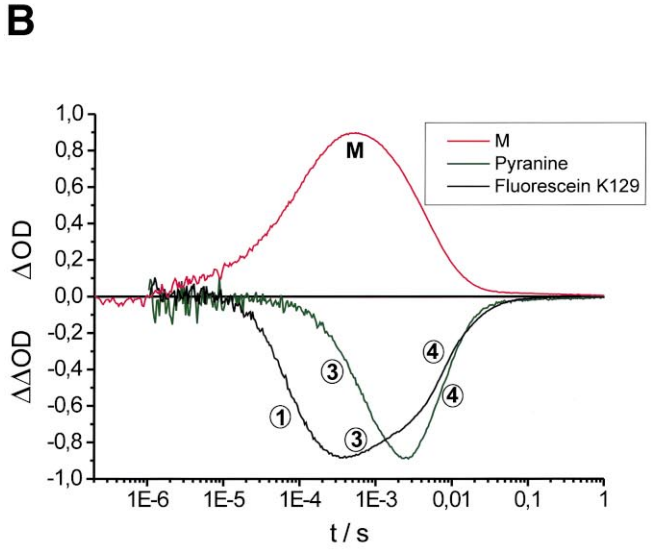
B
M
Pyranine
Fluorescein K129
ΔOD
ΔΔOD
t / s

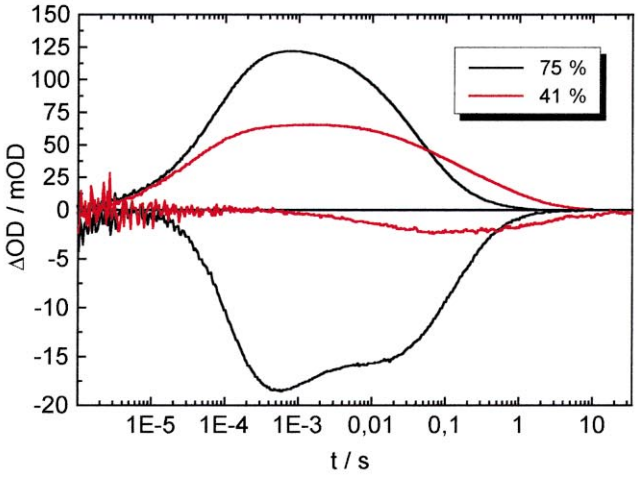
C
75 %
41 %
ΔOD / mOD
t / s

Fig. 1. Proton transfer reactions across bR and along the PM surface. (A) Sketch of bR molecules (RH^+, protonated Schiff base) in the PM with fluorescein (F) covalently bound to the amino acid K129 at the extracellular side and to C36 at the cytoplasmic side. Pyranine (P) resides in the aqueous bulk phase. Numbers refer to proton transfer reactions monitored by the respective optical pH probes. (B) Comparison of the time course of light-induced pH changes at the PM with rise and decay of the M intermediate. M was monitored as absorbance changes at 412 nm while bR-bound fluorescein and pyranine in the aqueous bulk phase were measured at 490 and 457 nm, respectively (aqueous PM suspension, 150 mM KCl, pH 7.1, 20°C; unpublished results by D. Rottschäfer and N.A.D.). Further experimental details and discussion of the data are presented in [5,8–10]. (C) Effect of hydration on the photocycle (M intermediate, upper traces) and pumping cycle (pyranine signal, lower traces) of bR in oriented PM films at 20°C (unpublished results by S. Verclas and N.A.D.).
←

observation that all protons pumped by bR are diffusing laterally along the membrane surface for long distances (several thousand Å; reaction 2 in Fig. 1A) before equilibrating into the aqueous bulk phase (reaction 3) [5,14]. Hydrogen ions move more slowly at the membrane-water interphase (diffusion coefficient $D_{app} = 1 \times 10^{-6}$ cm^2/s at 20°C; about 240 nm in 150 μs [5]) than in the aqueous bulk phase ($D = 9.3 \times 10^{-5}$ cm^2/s). However, due to the surprisingly slow surface to bulk transfer rate (about 1 ms; Fig. 1B, reaction 3) protons can laterally diffuse macroscopic distances along the PM. For PM in ice [8], or in the presence of mobile buffer molecules [3,10,36] pyranine responds to the ejected proton as fast as fluorescein bound to bR, demonstrating that the surface/bulk transfer is no longer rate limiting. Since the translational diffusion of water molecules is 4.4 times faster than the measured H^+ transfer rate along the surface, diffusing water molecules can act as vehicles. H^+ transfer along a membrane surface via water molecules could significantly contribute to, or even dominate, chemiosmotic energy coupling.

2. The low resolution structure of the M intermediate

For a complete understanding of the function of a protein like bR it is desirable to follow up structural changes in space and time with high resolution parallel to the working cycle. Since the intensity scattered from a single molecule is too low, taking into account the limits set by radiation damage, an ensemble of molecules has always to be considered. In this situation information about structural changes during the working cycle can be obtained in two ways, either by trapping intermediate states or by time-resolved detection of the scattered intensity after excitation. Both alternatives were successfully carried out in the case of bR.

2.1. Electron, neutron, and X-ray structures

Since the observation that one proton is translocated by bR to the extracellular side during the transition from L to M [1–6,8,14,36], the M intermediate was considered to be a key state in the pumping process. It was obvious that knowledge of the M state structure would give an insight into the mech-

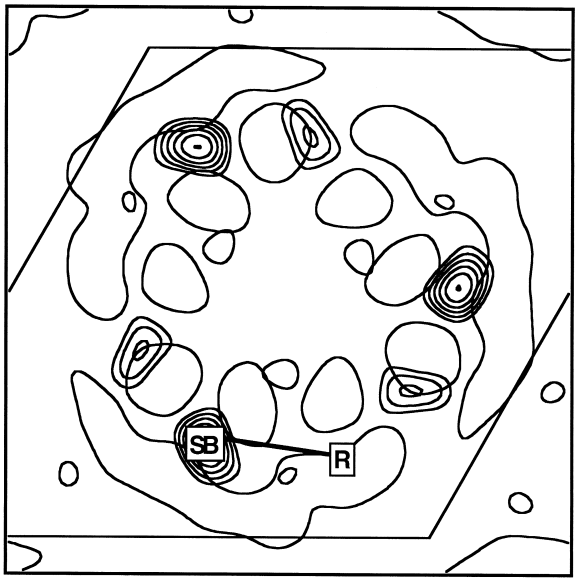

Fig. 2. $^2H_2O/H_2O$ difference density map at 15% r.h. (bold contour lines) showing the location of water molecules and exchangeable hydrogens in projection on the PM plane in the vicinity of the Schiff base (SB). The outline of three bR monomers and the position of the ring (R) of retinal are indicated. The in-plane position and orientation of the retinal are depicted according to neutron [46] and X-ray diffraction [65] experiments.

anism of proton translocation. One of the first attempts to visualize the M intermediate at low temperatures was performed by Glaeser et al. [37] using electron diffraction. The experiments showed no intensity changes in the resolution region from 60 to 5 Å and only small changes between 5 and 3.5 Å. It was assumed that proton pumping in bR is not accompanied by conformational alterations in the protein moiety. Neutron diffraction experiments were undertaken by Dencher et al. [38,39] with the aim to observe changes in the distribution of water molecules in M as compared to the ground state. As it was known that GuaHCl at high pH slows down the decay of the M state, wild-type PM films were soaked in a buffer containing GuaHCl at pH 9.4 and illuminated at +8°C. The films become yellow indicating the complete transformation to the M state, which was then preserved at liquid nitrogen temperatures. Neutron diffraction patterns of the ground state and of the M intermediate displayed clear differences in the reflection intensities of up to 9% in $\Sigma|\Delta I|/\Sigma I$ in the resolution region of 60–7 Å. By comparing diffraction patterns between films in H_2O and ^2H_2O it was derived that at least 80% of the differences resulted from changes in the protein structure and only a minor contribution could originate from a redistribution of water molecules. These observations indicate that small changes in the tertiary structure of bR take place during the photocycle. Significant density increase was observed near helix F and G and smaller alterations at helices B and D (Fig. 3A), which were interpreted as small changes in tilt angle of respective helices or as positional changes of amino acids [38,39]. These results were in contradiction to diffraction experiments by Glaeser et al. [37] and Nakasako et al. [40]. In their more recent studies the occurrence of conformational changes was confirmed and analysed in detail [41–43]. It was observed by optical spectroscopy that the bR mutant D96N is characterized by a large decrease in the decay rate of the M state with increasing pH [44]. Koch et al. [45] performed X-ray diffraction experiments on films of this mutant under continuous illumination at room temperature and pH 9.6. They found similar intensity changes between the BR and M state structures (Fig. 3B, 100% r.h.) as observed for wild-type (wt) bR in the neutron diffraction measurements mentioned above.

Neutron diffraction experiments with selectively deuterated retinals indicated that in the M state the polyene chain has tilted out of the plane of the membrane towards the cytoplasmic side by about 10° with only a minor movement of the β-ionone ring [46], in agreement with recent high resolution X-ray diffraction experiments [47,48].

2.2. Time-resolved X-ray diffraction on wt bR and the mutant D96N

To correlate structural changes with relaxation processes in the photo- and pumping cycle of bR, the structural transition from the M state to the ground state was followed by time-resolved X-ray diffraction using intense synchrotron radiation [9,45]. The changes in individual reflections before and immediately after the light flash are consistent both in amplitude and in direction with the steady-state experiments.

A comparison of these structural relaxation times at various environmental conditions with optical decay rates of intermediate states in the photocycle indicated that the observed structural changes relax during the transition from the N state to the ground state. In functional terms this means that the structural changes relax after the reprotonation of the Schiff base.

2.3. M accumulates in M_1 or M_2 depending on hydration

By time-resolved X-ray experiments only the relaxation of structural changes was followed. The onset of these changes could not precisely be attributed to photocycle intermediates. A first hint was obtained from X-ray diffraction experiments on the bR mutant D96N (pH 9.6) equilibrated at different relative humidities (15, 57, 75, and 100% r.h.) transformed to the M state by continuous illumination [20]. PM films at relative humidities $\geq 75\%$ showed the known changes in the tertiary structure (Fig. 3C), whereas films at r.h. $\leq 57\%$ r.h. displayed no changes in the difference density maps (Fig. 3D). These experiments demonstrated that two types of M states with and without structural changes compared to the ground state are existing. If one assumes that both M states would occur in the photocycle also at high hydration

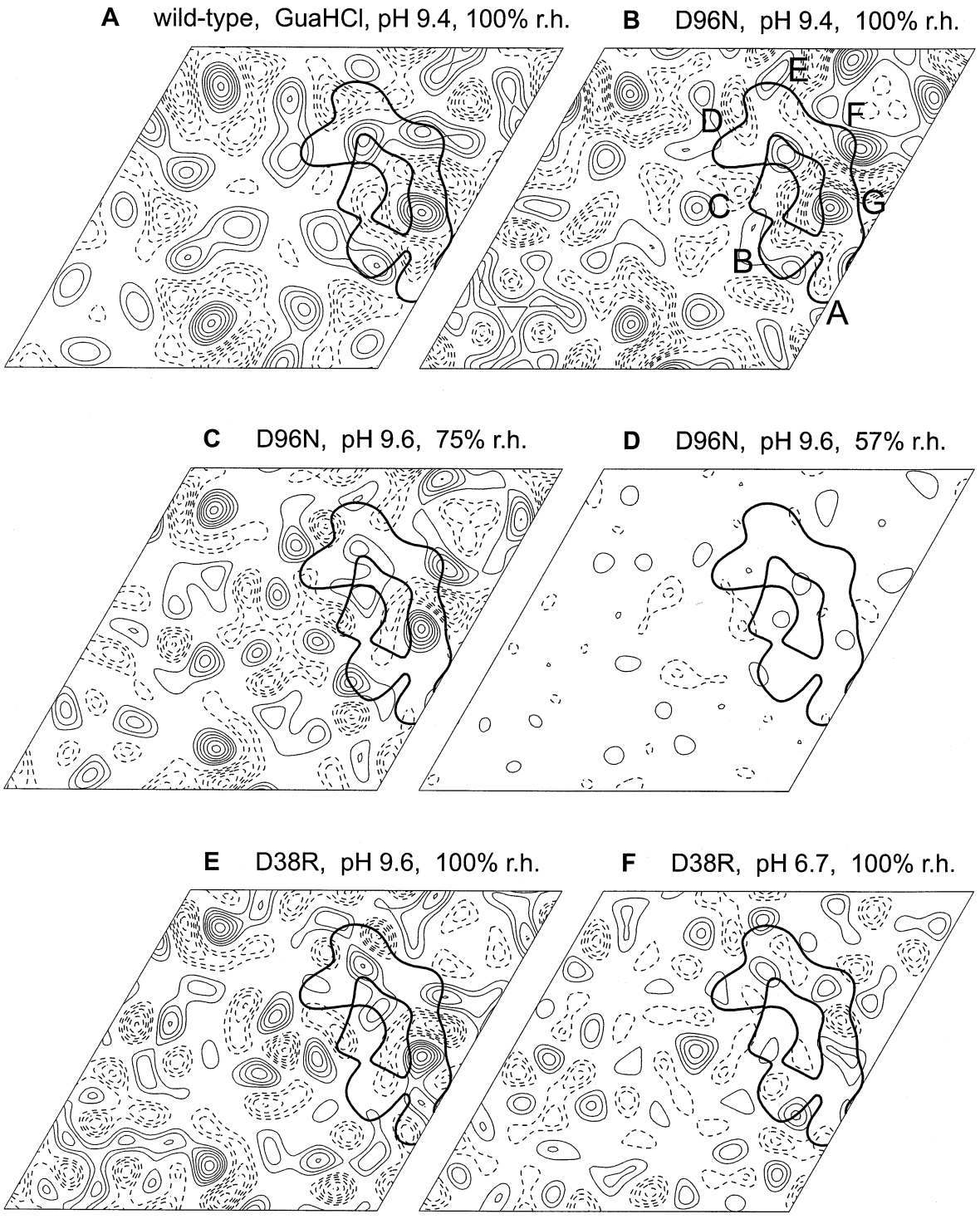

Fig. 3. Difference density maps (M minus BR state) of PM in projection: (A) from neutron diffraction on wt bR in 2 M GuaHCl in H_2O [39]; (B–D) from X-ray diffraction on the bR mutant D96N at three different hydrations [20,45]; (E,F) from X-ray diffraction on the bR mutant D38R at high and low pH [52]. The bold contour outlines the bR monomer; individual helices are marked by upper case letters from A to G. Continuous lines correspond to five positive, dashed lines to five negative equidistant density levels. Contour levels in different maps are scaled to each other.

but in a sequential order, the changes in the tertiary structure would develop within the M intermediate between M_1 and M_2 and would relax after the N state. Reconsidering the earlier experiments of Glaeser et al. [37] and Nakasako et al. [40], it seems now very probable that the M_1 intermediate was accumulated and therefore no changes in the tertiary structure were observed.

FT-IR measurements under identical conditions, although with much thinner PM films, verify that for all hydration levels the films were trapped in the M intermediate [20]. The distinction between L, M_1, M_2, M_N, and N intermediates was made upon the fingerprint region of the FT-IR difference spectra. The largest differences in the M state between the differently hydrated samples were found in the amide regions. Samples at hydration levels greater than 60% r.h. display the structural changes in the diffraction experiment and at the same time show in the amide I region a larger difference band at 1670 cm^{-1} than at 1660 cm^{-1} (M_2). On the other hand, the samples which do not show the changes in the tertiary structure (r.h. less than 60%) display a larger difference band at 1660 cm^{-1} than at 1670 cm^{-1} (M_1). These differences in the amide I region are also reflected in the amide II region, where the difference band at 1556 cm^{-1} is much larger in the more hydrated samples.

The concept of two M states was brought up from the evaluation of spectroscopic data in the visible wavelength region [49,50]. An irreversible step was assumed between M_1 and M_2 acting as a switch by changing the proton accessibility of the Schiff base from the extracellular to the cytoplasmic side and thus creating the vectoriality of the proton pump [50].

With respect to the function of bR, it was demonstrated that proton pumping occurs only in samples with hydration levels above 50–60% r.h. [29] (Fig. 1C). These results indicate that the observed structural changes are necessary for proton translocation and that at least part of these changes may form the switch, which changes the accessibility to the Schiff base [51].

2.4. Charge-controlled conformational changes

A hint for the origin of the conformational changes was given by the investigation of the bR mutant D38R [13,52]. X-ray diffraction experiments on samples at pH 6.7 do not show light-induced changes in the tertiary structure of bR to its full extent (Fig. 3F) whereas at pH 9.6 the characteristic structural changes were found (Fig. 3E). The interpretation of these experiments is that under illumination at pH 6.7 mainly the M_1 state is accumulated and the M_2 state at pH 9.6.

The substitution of the aspartic acid 38 by an arginine makes the charge pattern at the cytoplasmic side more positive. This new charge pattern in the mutant could interfere with the charge variation resulting from the deprotonation of the Schiff base and therefore slow down the large structural rearrangements. This would result in the accumulation of the M_1 state at neutral pH. At alkaline pH, another group on the cytoplasmic side might be deprotonated and compensates at least partly the added positive charge of the arginine. This would allow the structural changes associated with the transition to the M_2 state to take place.

The general conclusion also for wild-type bR can be drawn that a charge redistribution around the Schiff base and at the extracellular side of the molecule results in an altered force field within bR which drives the large structural changes [52].

3. The M state structure at high resolution elucidates the functional importance of water molecules

With the advent of the new concept for crystallization of bR in the lipidic cubic phase [53] high resolution ground state [54,55] and intermediate structures become available. Recently, Edman et al. [56] succeeded in solving the crystal structure of the early K intermediate and small structural changes with respect to the ground state BR could be resolved. Luecke at al. [48] trapped the late M state in crystals of the mutant D96N (PDB entries: 1c8r and 1c8s, release date: 20 October 1999). The advantage of this mutant is that a high amount of late M can be trapped at room temperature. The disadvantage is that, as indicated by the long decay time of M, the cytoplasmic proton translocation pathway is disturbed. To circumvent this disadvantage, the M_2 state in wild-type bR was accumulated to about

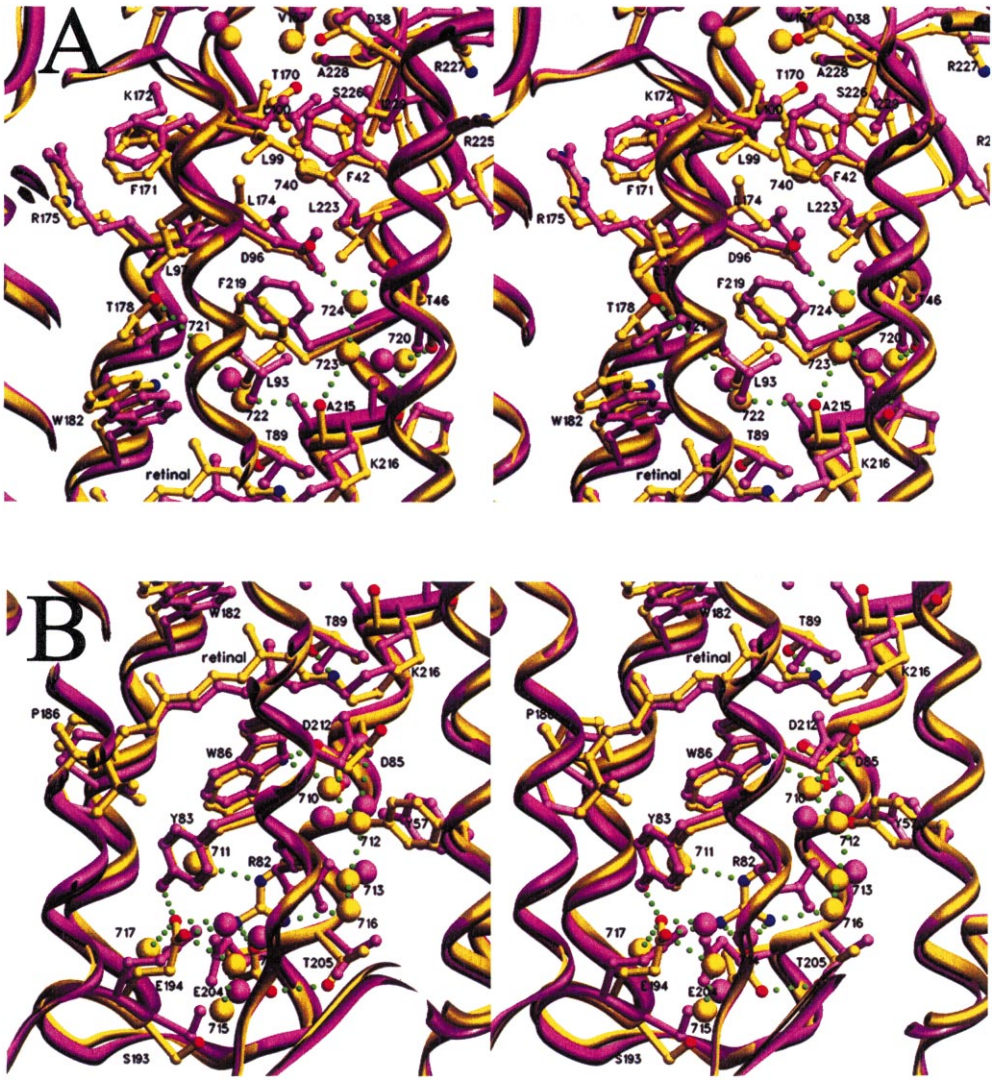

Fig. 4. Stereo images of atomic models of wt bR in the BR state (purple) and in the M state (yellow) from the cytoplasmic domain in A and the extracellular domain in B (PDB ID: 1cwq) [47]. Green dotted lines mark possible hydrogen bonds in the range between 2.4 and 3.7 Å for the M state model. Water molecules are displayed as purple and yellow balls for the BR and M state model, respectively. Only the water molecules of the M state structures are labelled.

35% and the crystal structure solved to 2.25 Å resolution (PDB ID: 1cwq, release date: 20 October 1999) [47]. It is obvious that both procedures to obtain information about late M have positive and negative consequences. The lower occupancy of 35% M_2 in the wild-type crystals leads to an increase of the noise in the density map for the M state. Both M state structures [47,48] show quite similar changes at the proton release side of bR. The striking features of the extracellular domain are the conformational changes in R82 and of the dyad E194/E204 in combination with displacements of water molecules (Fig. 4). It seems that after proton translocation from the Schiff base to D85 the effect of this movement of a positive charge results in a large downward reorientation of the positively charged R82 side chain towards the negatively charged dyad E194/E204. The switch function of R82 was predicted from theoretical considerations [57]. The change in the charge distribution and in the hydrogen bonding network should affect the pK values of the glutamic acid residues of the dyad so that a pro-

ton is released either directly from one of the glutamic acids or indirectly via a net of water molecules [12,28]. The 13-*cis* isomerization of the retinal with the SB nitrogen oriented upward towards T89, which in the ground state was hydrogen bonded to D85, the reorientation of D85, the downward displacement of the water molecule W710 and the reorientation of R82 (Fig. 4) leads to an isolation of the SB nitrogen from the new extracellular domain network of hydrogen bonds. Therefore, the reprotonation of the SB from the extracellular side in the late M state is improbable. Thus, one important element of the vectorial pump became visible.

Both structural M state models [47,48] do not provide a sufficiently clear picture of the proton pathway across the cytoplasmic domain. A common feature is the alteration in helices F and G, in line with the low resolution data [9,39,41,45,51], which result in an enlargement of cavities thereby enabling the inward and outward diffusion of water molecules. However, a continuous water-filled channel below or above the position of D96 is not seen. Therefore, the reprotonation of the Schiff base from D96 as well as the reprotonation of D96 itself is only possible by fluctuating water molecules and motions of amino acid side chains, as previously suggested by Dencher et al. [58,59].

The reorientations also allow new hydrogen bonds in the cavity between D96 and K216. Two further water molecules, W723 and W724, appear in the M state structure (Fig. 4A). W724 interacts with $O\delta_1$ of D96 and $O\gamma_1$ of T46 which had been in hydrogen bond contact in BR. W723 is in contact with W724, W720, and the carbonyl oxygen of A215. Thus W723 is strongly fixed in its position in contrast to the results for the D96N mutant [48]. We think this water is of importance for proton transport through the cytoplasmic part. Together these water molecules could form a proton transfer chain from D96 → W724 → W723 → O-A215 → W722 → SB. Only the remaining gap between W722 and SB of 5.8 Å is too large for a direct proton transfer. We suggest that this water molecule, since it is less stabilized than the next neighbour water molecules, can fluctuate to the Schiff base when the proton has reached the carbonyl oxygen region of A215 through the more stable water chain above.

The reprotonation pathway of D96 from the cytoplasmic surface seems to be different from what has been observed in other parts of the molecule. Here a density in the larger cavity formed in the M state is attributed to a water molecule (W740) which is surrounded by mostly hydrophobic residues (T170, F42, L100, L223, I229). The assignment of this density to a water molecule, which has no hydrogen bonding partners in its vicinity, is crystallographically quite unusual. However, it seems not improbable that an hydrophobic cavity can trap a water molecule. W740 has a distance of 5.35 Å to D96. This cavity has a narrow opening to the cytoplasmic surface formed by the nonpolar parts of the residues (A228, T170, L100, I229, S226). The higher flexibility and the partial opening in this part of the molecule may allow from time to time a water molecule to penetrate into this hydrophobic area. In this way, the contact to D96 might be achieved by a fluctuating water molecule and not by a continuous water channel. These results, in line with low resolution diffraction data [30], exclude that structural changes in the M state lead to a large increase in the number (11–20) of water molecules in the proton channel as previously proposed [60,61].

4. Thermal equilibrium fluctuations 'lubricate' transitions between intermediates

The kinetics of the photocycle is determined by energy barriers which need to be surmounted during subsequent steps between the different intermediate states. In particular in the case of charge displacements and conformational changes, thermal equilibrium fluctuations provide a kind of 'stochastic driving force' to overcome these barriers. With respect to the microsecond and millisecond time regime, determining the transition rates between intermediates (with the exception of the early J and K intermediates), even faster picosecond fluctuations play a major role for the intermediate transitions. A powerful tool to study dynamical properties of biological systems in a time range from 10^{-9}–10^{-14} s is given by the incoherent neutron scattering (INS) [32]. Because the neutrons are scattered mainly at more or less homogeneously distributed hydrogens in the sample, the hydrogen nuclei serve as probes to monitor the 'overall fluctuations' of the investigated structures.

4.1. Temperature and hydration control bR function via equilibrium fluctuations

Environmental conditions, like temperature and the hydration level (Fig. 1C), have a distinct influence on the kinetics of the photocycle and on proton pumping [21,24,62]. On the other hand, the temperature and the amount of solvent molecules surrounding biological macromolecules strongly determine dynamical properties [63]. Since the equilibrium fluctuations are not only influenced by temperature but also by the hydration level, a reduced quasi-elastic incoherent structure factor is observed due to 'dehydration by cooling' [31]. The influence of temperature on the dynamical behaviour of samples at different initial hydration levels is shown in Fig. 5. Regarding the equilibrium fluctuations at particular temperatures where the individual intermediate states are trapped (Fig. 5) the following relation between photocycle kinetics and dynamical properties evolves: the first part of the photocycle ($bR \rightarrow J \rightarrow K \rightarrow L$) seems not to be significantly influenced by large amplitude fluctuations. Therefore, the change of residue K216 in helix G reported for the K state [56] is not caused by large amplitude thermal fluctuations but a consequence of the local stress exerted on the backbone hydrogen bonds due to retinal isomerization together with the K216 structural alterations. It appears that the 'quantity' of large amplitude fluctuations is rate-limiting for transitions between the intermediates of the second half of the photocycle. The prominent tertiary structural change [39,45] which occurs during the $M_1 \rightarrow M_2$ transition is inhibited below 230 K and at hydration levels below $h = 0.18$ [20]. Above 250 K a significant deviation in the 'quantity' of large amplitude fluctuations for different hydration levels is observed (Fig. 5). Therefore, reduced large amplitude fluctuations seem to be responsible for prolonged or hindered transitions ($M_1 \rightarrow M_2$ and $M_2 \rightarrow N \rightarrow O \rightarrow bR$) [24] and disable tertiary structural changes at low temperatures and at low hydration levels [20]. The difference in the dynamical properties is largest above $T = 260$ K and decay rates of the M intermediate are prolonged by one order of magnitude when lowering the hydration level from $h = 0.38$ to 0.18 [24] (see also Fig. 1C). This indicates that in particular the M decay and the relaxation back to the ground state need a considerable 'quantity' of large amplitude picosecond fluctuations to 'lubricate' conformational relaxation of the protein scaffold on the millisecond time scale.

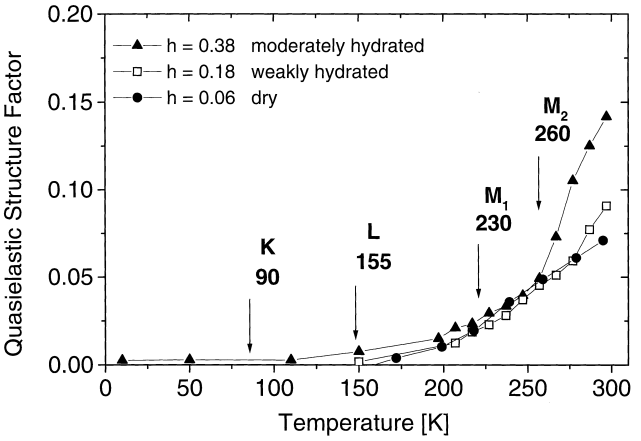

Fig. 5. Temperature dependence of the quasi-elastic incoherent structure factor of PM samples at different hydration levels (h, weight water per weight PM; data from [63]). For the intermediates K, L, M_1 and M_2 the corresponding trapping temperatures are indicated.

4.2. Water molecules at lipid head groups modulate bR flexibility and function

The influence of lipids in the PM on the dynamical and functional properties of bR was investigated by comparing the natural purple membrane composed of 75% bR (w/w) and 25% lipid (w/w) and a partially delipidated PM having only 10% lipids (w/w) [24]. With both types of membranes measurements have been performed using moderately and weakly hydrated ($h = 0.38$ and $h = 0.18$, respectively) samples. The difference in flexibility between both types of membranes is relatively small in the case of weakly hydrated samples and more pronounced in the case of moderately hydrated samples. As already known from results given before, a more complete hydration is related to an increased internal flexibility (Fig. 5). This effect is more pronounced in the case of natural PM samples as compared to delipidated PM samples.

The fact that the differences in the flexibility between natural and delipidated PM samples are much more pronounced in more completely hydrated samples gives strong evidence that mainly the presence of hydration water, which is attached to the polar lipid head groups at high hydration levels [28,30,64], in-

creases the internal flexibility of the protein-lipid complex [32]. The impressive accordance of the observed dynamical properties with the time constant characterizing the M decay [24] demonstrates that restricted internal flexibility is related to prolonged M decay. Therefore, one of the outstanding properties of lipids in the PM seems to be that mainly these lipids attract solvent molecules ensuring a sufficient structural flexibility of the whole PM, which is essential for a proper function of bR.

5. Concluding remarks

Bacteriorhodopsin is a superb system to elucidate the functional importance of water in membranes. In fact, besides the water-soluble protein myoglobin, bR is the best understood protein in respect to the hydration dependence of function and dynamics, as well as to the properties of the hydration water. From all the data gathered, the importance of water molecules for the function, structure, and dynamics of bR and the PM is established. Water molecules are key elements of the proton transport mechanism by providing a proton pathway and proton acceptor/donor groups. In addition, water molecules 'lubricate' the picosecond molecular motions and the light-triggered micro- to millisecond tertiary structural changes of the protein. With the advent of high resolution structures of photocycle intermediates, such as of the M state(s), the detection of photon-induced rearrangement of water molecules and hydrogen bonds concomitant with the conformational changes in the chromophore and the protein moiety is feasible. This will be a clue for understanding vectorial proton transport by bR at the atomic level. Last but not least, the hydration water at the membrane surface with its peculiar properties participates in long range proton transfer, mediating bioenergetic coupling between the proton source bR and a sink, e.g., the H^+-ATP synthase or the flagellar motor.

Acknowledgements

We thank J. Fitter, B. Gehrmann, J. Heberle, D. Hehn, D. Rottschäfer, and S. Verclas for their help with the figures and the content of the paper. This work was supported by grants of EU-BIOTECH and the Deutsche Forschungsgemeinschaft Sfb 189 to G.B and Sfb 472 to N.A.D. as well as the grants of the BMBF (03-DE4DAR-18) and the Fonds der Chemischen Industrie.

References

[1] N. Dencher, M. Wilms, Biophys. Struct. Mech. 1 (1975) 259–271.
[2] R.H. Lozier, R.A. Bogomolni, W. Stoeckenius, Biophys. J. 15 (1975) 955–962.
[3] S. Grzesiek, N.A. Dencher, FEBS Lett. 208 (1986) 259–271.
[4] D. Oesterhelt, B. Hess, Eur. J. Biochem. 37 (1973) 316–326.
[5] J. Heberle, J. Riesle, G. Thiedemann, D. Oesterhelt, N.A. Dencher, Nature 370 (1994) 379–382.
[6] S. Grzesiek, N.A. Dencher, Proc. Natl. Acad. Sci. USA 85 (1988) 9509–9513.
[7] N.A. Dencher, M.P. Heyn, FEBS Lett. 108 (1979) 307–310.
[8] J. Heberle, N.A. Dencher, FEBS Lett. 277 (1990) 277–280.
[9] N.A. Dencher, J. Heberle, C. Bark, M.H.J. Koch, G. Rapp, D. Oesterhelt, K. Bartels, G. Büldt, Photochem. Photobiol. 54 (1991) 881–887.
[10] J. Heberle, N.A. Dencher, Proc. Natl. Acad. Sci. USA 89 (1992) 5996–6000.
[11] Y. Cao, L.S. Brown, J. Sasaki, A. Maeda, R. Needleman, J.K. Lanyi, Biophys. J. 68 (1995) 1518–1530.
[12] R. Rammelsberg, G. Huhn, M. Lübben, K. Gerwert, Biochemistry 37 (1998) 5001–5009.
[13] J. Riesle, D. Oesterhelt, N.A. Dencher, J. Heberle, Biochemistry 35 (1996) 6635–6643.
[14] U. Alexiev, R. Mollaaghababa, P. Scherrer, H.G. Khorana, M.P. Heyn, Proc. Natl. Acad. Sci. USA 92 (1995) 372–376.
[15] E. Nachliel, M. Gutman, S. Kiryati, N.A. Dencher, Proc. Natl. Acad. Sci. USA 93 (1996) 10747–10752.
[16] S. Checover, E. Nachliel, N.A. Dencher, M. Gutman, Biochemistry 36 (1997) 13919–13928.
[17] L.S. Brown, R. Needleman, J.K. Lanyi, Biochemistry 38 (1999) 6855–6861.
[18] R. Korenstein, B. Hess, Nature 270 (1977) 184–186.
[19] G. Varo, L. Keszthelyi, Biophys. J. 47 (1985) 243–246.
[20] H.J. Sass, I.W. Schachowa, G. Rapp, M.H. Koch, D. Oesterhelt, N.A. Dencher, G. Büldt, EMBO J. 16 (1997) 1484–1491.
[21] G. Thiedemann, J. Heberle, N.A. Dencher, in: J.L. Rigaud (Ed.), Structures and Functions of Retinal Proteins, John Libbey Eurotext Ltd., 1992, pp. 217–220.
[22] P. Hildebrandt, M. Stockburger, Biochemistry 23 (1984) 5539–5548.
[23] G. Varo, J.K. Lanyi, Biophys. J. 59 (1991) 313–322.
[24] J. Fitter, S.A. Verclas, R.E. Lechner, H. Seelert, N.A. Dencher, FEBS Lett. 433 (1998) 321–325.
[25] A. Maeda, J. Sasaki, Y. Shichida, T. Yoshizawa, Biochemistry 31 (1992) 462–467.

[26] W.B. Fischer, S. Sonar, T. Marti, H.G. Khorana, K.J. Rothschild, Biochemistry 33 (1994) 12757–12762.
[27] A. Maeda, J. Sasaki, Y. Yamazaki, R. Needleman, J.K. Lanyi, Biochemistry 33 (1994) 1713–1717.
[28] G. Papadopoulos, N.A. Dencher, G. Zaccai, G. Büldt, J. Mol. Biol. 214 (1990) 15–19.
[29] T. Hauss, G. Papadopoulos, S.A.W. Verclas, G. Büldt, N.A. Dencher, Physica 236 (1997) 217–219.
[30] M. Weik, G. Zaccai, N.A. Dencher, D. Oesterhelt, T. Hauss, J. Mol. Biol. 275 (1998) 625–634.
[31] R.E. Lechner, J. Fitter, N.A. Dencher, T. Hauss, J. Mol. Biol. 277 (1998) 593–603.
[32] J. Fitter, R.E. Lechner, N.A. Dencher, J. Phys. Chem. B 103 (1999) 8036–8050.
[33] R.E. Lechner, N.A. Dencher, J. Fitter, Th. Dippel, Solid State Ionics 70/71 (1994) 296–304.
[34] R.E. Lechner, N.A. Dencher, J. Fitter, G. Büldt, A.V. Belushkin, Biophys. Chem. 49 (1994) 91–99.
[35] S. Grzesiek, N.A. Dencher, Biophys. J. 50 (1986) 265–276.
[36] L.A. Drachev, A.D. Kaulen, V.P. Skulachev, FEBS Lett. 178 (1984) 331–335.
[37] R.M. Glaeser, J. Baldwin, T.A. Ceska, R. Henderson, Biophys. J. 50 (1986) 913–920.
[38] N.A. Dencher, D. Dresselhaus, G. Maret, G. Papadopoulos, G. Zaccai, G. Büldt, in: Proceedings of the Yamada Conference XXI, 1988, pp. 109–115.
[39] N.A. Dencher, D. Dresselhaus, G. Zaccai, G. Büldt, Proc. Natl. Acad. Sci. USA 86 (1989) 7876–7879.
[40] M. Nakasako, M. Kataoka, F. Tokunaga, Y. Amemiya, in: Proceedings of the Yamada Conference XXI, 1988, pp. 323–324.
[41] T. Oka, H. Kamikubo, F. Tokunaga, J.K. Lanyi, R. Needleman, M. Kataoka, Biophys. J. 76 (1999) 1018–1023.
[42] H. Kamikubo, T. Oka, Y. Imamoto, F. Tokunaga, J.K. Lanyi, M. Kataoka, Biochemistry 36 (1997) 12282–12287.
[43] B.G. Han, J. Vonck, R.M. Glaeser, Biophys. J. 67 (1994) 1179–1186.
[44] H.J. Butt, K. Fendler, E. Bamberg, J. Tittor, D. Oesterhelt, EMBO J. 8 (1989) 1657–1663.
[45] M.H.J. Koch, N.A. Dencher, D. Oesterhelt, H.J. Plöhn, G. Rapp, G. Büldt, EMBO J. 10 (1991) 521–526.
[46] T. Hauss, G. Büldt, M.P. Heyn, N.A. Dencher, Proc. Natl. Acad. Sci. USA 91 (1994) 11854–11858.
[47] H.J. Sass, G. Büldt, D. Neff, R. Gessenich, D. Hehn, R. Schlesinger, J. Berendzen, P. Ormos, Nature (2000) in press.
[48] H. Luecke, B. Schobert, H.T. Richter, J.P. Cartailler, J.K. Lanyi, Science 286 (1999) 255–261.
[49] B. Hess, D. Kuschmitz, FEBS Lett. 74 (1977) 29–34.
[50] G. Varo, J.K. Lanyi, Biochemistry 29 (1990) 2241–2250.
[51] S. Subramaniam, I. Lindahl, P. Bullough, A.R. Faruqi, J. Tittor, D. Oesterhelt, L. Brown, J. Lanyi, R. Henderson, J. Mol. Biol. 287 (1999) 145–161.
[52] H.J. Sass, R. Gessenich, M.H. Koch, D. Oesterhelt, N.A. Dencher, G. Büldt, G. Rapp, Biophys. J. 75 (1998) 399–405.
[53] E.M. Landau, J.P. Rosenbusch, Proc. Natl. Acad. Sci. USA 93 (1996) 14532–14535.
[54] E. Pebay-Peyroula, G. Rummel, J.P. Rosenbusch, E.M. Landau, Science 277 (1997) 1676–1681.
[55] H. Luecke, B. Schobert, H.T. Richter, J.P. Cartailler, J.K. Lanyi, J. Mol. Biol. 291 (1999) 899–911.
[56] K. Edman, P. Nollert, A. Royant, H. Belrhali, E. Pebay-Peyroula, J. Hajdu, R. Neutze, E.M. Landau, Nature 401 (1999) 822–826.
[57] C. Scharnagl, S.F. Fischer, Chem. Phys. 212 (1996) 231–246.
[58] N.A. Dencher, J. Heberle, G. Büldt, H.-D. Höltje, M. Höltje, in: J.L. Rigaud (Ed.), Structures and Functions of Retinal Proteins, John Libbey Eurotext Ltd., 1992, pp. 213–216.
[59] N.A. Dencher, J. Heberle, G. Büldt, H.-D. Höltje, M. Höltje, in: Pulman et al. (Ed.), Membrane Proteins: Structures, Interactions and Models, Kluwer Academic, 1992, pp. 69–84.
[60] P.J. Schulenberg, W. Gärtner, S.E. Braslavsky, J. Phys. Chem. 99 (1995) 9617–9624.
[61] G. Varo, J.K. Lanyi, Biochemistry 34 (1995) 12161–12169.
[62] T. Iwasa, F. Tokunaga, T. Yoshizawa, Biophys. Struct. Mech. 6 (1980) 253–270.
[63] J. Fitter, R.E. Lechner, N.A. Dencher, Biophys. J. 73 (1997) 2126–2137.
[64] P.K. Rogan, G. Zaccai, J. Mol. Biol. 145 (1981) 281–284.
[65] G. Büldt, K. Konno, K. Nakanishi, H.J. Plöhn, B.N. Rao, N.A. Dencher, Photochem. Photobiol. 54 (1991) 873–879.